Materials Advances

ROYAL SOCIETY OF CHEMISTRY

PAPER

View Article Online
View Journal | View Issue

Cite this: *Mater. Adv.*, 2023, 4, 3628

A semiconducting supramolecular novel Ni(II)-metallogel derived from 5-aminoisophthalic acid low molecular weight gelator: an efficient Schottky barrier diode application†

Baishakhi Pal,‡[a] Subhendu Dhibar,‡*[b] Ritam Mukherjee,[b] Subham Bhattacharjee,[c] Partha Pratim Ray *[a] and Bidyut Saha *[b]

Received 22nd May 2023,
Accepted 16th July 2023

DOI: 10.1039/d3ma00260h

rsc.li/materials-advances

An outstanding approach for the development of a supramolecular metallogel with nickel(II) ion and 5-aminoisophthalic acid as a gelator (LMWG) in DMF medium has been accomplished at room temperature. Rheological studies of the supramolecular Ni(II)-metallogel established the mechanical compactness of the gel material. FESEM microstructural study and EDX elemental mapping showed flake-like morphological patterns and major chemical constituents of the Ni(II)-metallogel. The possible metallogel formation approach has been examined using FT-IR spectroscopic study. Moreover, the supramolecular Ni(II)-metallogel assemblies show electrical conductivity in metal–semiconductor (MS) junction electronic devices. The metallogel based thin film device shows an electrical conductivity of 1.53×10^{-5} S m^{-1}. Semiconductor properties such as Schottky barrier diode nature of the synthesized Ni(II)-metallogel based devices were explored.

1. Introduction

Gels are often thought to consist of an elastic cross-linked network containing a trapped liquid.[1] Gels are ubiquitous in daily life; notable examples are hair gels, toothpaste, and soft contact lenses. The field of materials science and its associated industrial applications are constantly being reinforced by molecular self-assembly, one of the main branches of supramolecular chemistry.[2] The spontaneous self-assembly of molecules produces three-dimensional frameworks known as supramolecular gels.[3] The gelators and solvent molecules, which are immobilised by the gelator molecules in the 3D soft gel scaffolds, are the two principal elements making up the supramolecular gel.[4] The vial inversion test, which demonstrates that a vial of gel remains stable against gravity, provides the most direct primary evidence of gel formation.[5] The organic and/or inorganic gelators trap various solvents, such as water (H_2O),[6] acetonitrile (H_3C–C≡N),[7] ethanol (CH_3CH_2OH),[8] methanol (CH_3OH),[9] dichloromethane (CH_2Cl_2),[10] deuterated dichloromethane (CD_2Cl_2),[11] 1,2-dichlorobenzene ($C_6H_4Cl_2$),[12] acetone (CH_3COCH_3),[13] carbon tetrachloride (CCl_4),[14] DMF ($(CH_3)_2NC(O)H$),[15] tetrahydrofuran ($(CH_2)_4O$),[16] dimethyl sulfoxide (C_2H_6OS),[17] and toluene ($C_6H_5CH_3$),[18] to create three-dimensional gel structures.[19] Polymers, such as polyester, poly(ethylene glycol), polyolefins, polycaprolactones, and polycarbonates, often serve as gelators to produce a variety of stable gel compositions.[20] However, low molecular weight gelators (LMWGs), which have molecular weights under 3000, have a strong capacity in supramolecular gel formation through the immobilization of solvent molecules.[21,22] Literature is full with various low molecular weight gelators, such as alkenes,[23] amides,[24] modified amino acids,[25] urea,[26] peptides,[27] sugars,[28] and dendrimers,[29] which have wonderful gelation properties in the presence of different solvent molecules. Supramolecular gel formation is the output of intriguing non-covalent interactions, including hydrogen bonds,[30] electrostatic interactions,[31] hydrophobic[32] and hydrophilic forces,[33] van der Waals forces,[30] and aryl-system-based interactions.[34] Supramolecular gels have become a vital area in materials science owing to their numerous applications in both the academic and industrial arena, such as catalysis,[6a,b,35] lithography,[36] opto-electronic devices,[37] electrochemical devices,[38] chemo-sensors,[39] cell culture,[40] drug delivery,[41] tissue engineering,[42] and semiconductors.[15]

[a] *Department of Physics, Jadavpur University, Jadavpur, Kolkata-700032, India. E-mail: parthap.ray@jadavpuruniversity.in; Tel: +91 3324572844*
[b] *Colloid Chemistry Laboratory, Department of Chemistry, The University of Burdwan, Golapbag, Burdwan-713104, West Bengal, India. E-mail: sdhibar@scholar.buruniv.ac.in, bsaha@chem.buruniv.ac.in; Tel: +91 7001575909, +91 9476341691*
[c] *Department of Chemistry, Kazi Nazrul University, Asansol-713303, West Bengal, India*

† Electronic supplementary information (ESI) available. See DOI: https://doi.org/10.1039/d3ma00260h

‡ BP and SD should be treated as joint first authors

Metallogels are a significant class of supramolecular gels, which are formed by the incorporation of metal ions with appropriate LMWG to create a 3D supramolecular soft gel structure, which may exhibit intriguing and unusual features.[5] In metallogels, metal ions impart a number of significant functionalities into the metallogel scaffolds, including redox activity,[43] magnetic behaviour,[44] conductivity,[45] actuators,[46] catalytic activity,[47] optical activity.[48] As smart functional materials, supramolecular metallogel systems based on transition metals have recently received interest owing to their affordability and availability. Researchers have recognized several useful metallogels of transition metal ions, such as Co(II),[49–51] Ni(II),[51,52] Cu(II),[15d,e,g] Cd(II),[15a] Fe(II/III),[53–55] Zn(II),[15h,i] Mn(II),[5] with strong applications in science.[56] However, metallogels with Ni(II)-ion have important applications in fluorescence switching,[57] electrocatalysis,[58] non-linear property,[59] self-healing,[60] semiconducting devices,[52] catalysis,[61] and magnetic materials.[62] Recently, Dhibar *et al.* have reported different metallogel-mediated metal–semiconductor (MS) junction device for Schottky barrier diode application. Metallogel-based Schottky diodes are highly significant in various applications for several reasons. First, metallogels offer tunable electronic properties that can be customized by selecting specific metals and ligands during synthesis. This tunability allows for precise control over the energy band structure and electronic behavior of the Schottky diode, enabling the creation of tailored device characteristics. Second, metallogels exhibit excellent stability, ensuring the long-term performance and reliability of Schottky diodes. Their robust structure and resistance to degradation make them suitable for deployment in diverse environments and applications. Third, metallogels can be fabricated using a range of techniques, including solution processing, self-assembly, and templating methods. This versatility in fabrication enables compatibility with various substrates and facilitates scalable production, facilitating the integration of metallogel-based Schottky diodes into different electronic devices. Furthermore, metallogels can be easily integrated with other electronic components, such as transistors and sensors, owing to their compatibility with different materials and fabrication techniques. This seamless integration allows for the development of multifunctional devices and systems with enhanced performance and expanded functionality. Overall, metallogel-based Schottky diodes offer a unique combination of tunable electronic properties, stability, versatile fabrication methods, tailored surface properties, and compatibility with other electronic components. These characteristics make them indispensable for a wide range of electronic applications, where precise control over device properties and reliable performance are paramount. Following the trend, herein, we have demonstrated the synthetic procedure of a room temperature stable metallogel of nickel(II)-ion and 5-aminoisophthalic acid as a LMWG in DMF medium (Fig. 1) for tunable, stable electronic device fabrication. The vial inversion test of the Ni(II)-metallogel (*i.e.* Ni@5AIA) shows the stability of Ni@5AIA gel against the gravitational force (Fig. 1). The mechanical property and morphological patterns have been established. With the aim of achieving the capability of the metallogel based metal–semiconductor (MS) junction device, we succeeded in fabricating a Schottky barrier diode (SD).

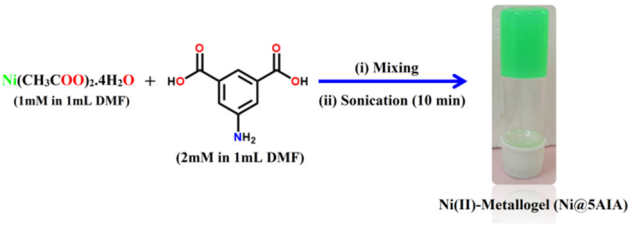

Fig. 1 Synthetic procedure of gelation and photographic image of Ni(II)-metallogel (Ni@5AIA).

2. Experimental

2.1. Materials

Nickel(II) acetate tetrahydrate (98%) and 5-aminoisophthalic acid (94%) were purchased from Sigma-Aldrich and used as received. Dry solvents (*i.e. N*,*N*-dimethyl formamide (DMF) was used for the entire study).

2.2. Apparatus and measurements

A Shimadzu UV-3101PC spectrophotometer was used to collect UV-Vis absorption spectral data.

Rheology experiments of the gel were done using an Anton Paar 100 rheometer with a cone and plate geometry (CP 25-2). All the mechanical measurements were done by fixing the gap distance between the cone and the plate at 0.05 mm. The gels were scooped onto the plate of the rheometer. An oscillatory strain amplitude sweep experiment was performed at a constant oscillation frequency of 1 Hz for the applied strain range 0.001–10% at 20 °C.

Microstructural features were analysed using a Carl Zeiss SUPRA 55 VP FESEM instrument. The ZEISS, EVO 18 apparatus was used to perform EDX elemental mapping studies.

A Shimadzu FTIR-8400S made FTIR spectrometer was used for IR spectroscopy.

A digital gel melting point measurement apparatus (Aplab MPA-01) was used to test the T_{gel} of the Ni@5AIA metallogel.

Keithley 2401 sourcemeter interfaced with a computer was used to perform the current–voltage (*I*–*V*) characteristics studies of our synthesized metallogel material based thin film device.

2.3. Synthetic procedure of Ni(II)-metallogel (Ni@5AIA)

A greenish-yellow colour stable Ni(II)-metallogel (Ni@5AIA) was synthesized by a one shot mixing of 1 mL DMF solution of nickel(II) acetate tetrahydrate (0.248 g, 1 mmol) and 1 mL DMF solution of 5-aminoisophthalic acid (0.362 g, 2 mmol) followed by the continuous sonication of the mixture for 10 minutes at room temperature (Fig. 1). The vial inversion test of Ni@5AIA metallogel proved its stability against the gravitational force (Fig. 1). The minimum critical gelation concentration (MGC) of Ni@5AIA metallogel was recorded at ~610 mg mL^{-1}. The concentrations of $Ni(CH_3COO)_2{\cdot}4H_2O$ and 5-aminoisophthalic

acid were varied in a certain range (*i.e.* 30–610 mg mL^{-1}) to evaluate the MGC of Ni@5AIA metallogel. Herein, the ratio of the Ni@5AIA metallogel forming components was maintained as [$Ni(CH_3COO)_2{\cdot}4H_2O$]: [5-aminoisophthalic acid] = 1 : 2, (w/w). The greenish-yellow colour stable Ni@5AIA metallogel was obtained at 610 mg mL^{-1} concentration of Ni(II)-acetate salt and 5-aminoisophthalic acid in DMF solvent. The gel melting temperature (T_{gel}) of Ni@5AIA metallogel was recorded as 120 °C ± 2 °C *via* a digital melting-point measuring apparatus. The stability of the Ni@5AIA metallogel in various pH media was also assessed, and the specific details can be found in the ESI.†

3. Results and discussion

3.1. Rheological analysis

The mechanical properties of the Ni@5AIA metallogel were characterized using a rheometer instrument of angular frequency and strain-sweep measurement. The higher values of storage modulus (G') than loss modulus (G'') confirm the sample as gel material. Rheological investigation proved that G' of Ni@5AIA metallogel is noticeably higher than that of G'' maintaining at a definite concentration of $Ni(CH_3COO)_2{\cdot}4H_2O$ and 5-aminoisophthalic acid (*i.e.* MGC = 610 mg mL^{-1}) (Fig. 2).

The rheological data of Ni@5AIA shows $G' > G''$, which establishes the gel nature with semi-solid like performance. The average storage modulus of Ni@5AIA metallogel (*i.e.* $G' > 10^4$ Pa) was detected to be significantly higher than the loss modulus (G'') in favour of the considerable endurance limit of Ni@5AIA metallogel (Fig. 2).

Fig. 3 depicts a strain-sweep experiment on Ni@5AIA metallogel material at a constant frequency of 6.283 rad s^{-1}. Results from the strain-sweep experiment show that the critical strain, the lowest strain for gel breakdown of Ni@5AIA metallogel, occurs at a strain of 0.45% when G' mixes with G'' (Fig. 3).

3.2. Microstructural study

The FESEM microstructural pattern of the Ni@5AIA reveals a flake-like hierarchical network (Fig. 4a and b).

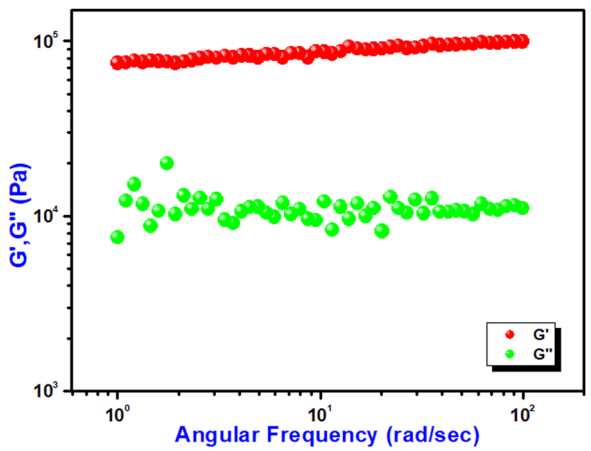

Fig. 2 Angular frequency measurements *vs.* G' and G'' of Ni@5AIA metallogel.

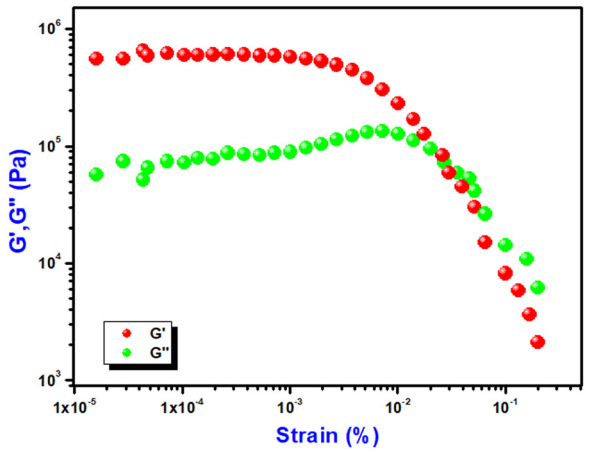

Fig. 3 Strain-sweep measurements of Ni@5AIA metallogel performed at a constant frequency of 6.283 rad s^{-1}.

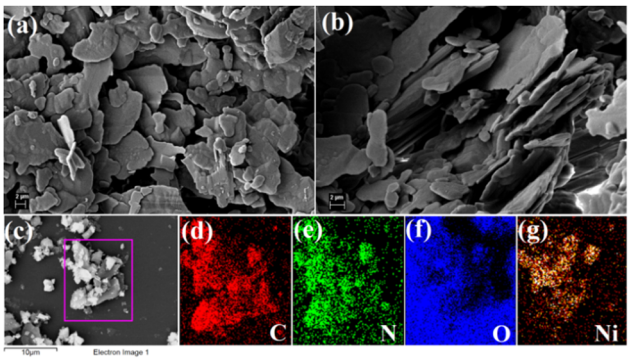

Fig. 4 (a) and (b) FESEM microstructural pattern of Ni@5AIA metallogel. Chemical compositions by EDS are shown in (c)–(g).

The FESEM structural arrangements of the Ni@5AIA metallogel were formed due to the combination of $Ni(OAc)_2{\cdot}4H_2O$ and 5-aminoisophthalic acid in DMF medium over continuous sonication. EDX elemental mapping confirms the presence of C, N, O, and Ni elements of $Ni(OAc)_2{\cdot}4H_2O$, 5-aminoisophthalic acid, and DMF molecules, accountable for the Ni@5AIA metallogel network formation (Fig. 4c–g).

3.3. FT-IR spectral analysis

The FT-IR spectral data of Ni@5AIA metallogel in xerogel form unveils the key peaks located at 3320–3150, 2940, 1650, 1370, and 1108 cm^{-1} for OH stretching, –CH stretching, C═O (carboxylic) stretching, $–CH_3$, vs(COO), respectively, and additional peaks centered at 402 cm^{-1} attributed to Ni–O stretching vibrations (Fig. 5). FT-IR spectral data displays the supramolecular interactions in Ni@5AIA metallogel among the metallogel forming chemical components.

3.4. Fabrication of thin film device

The Schottky device for the gel was made in a sandwich configuration with ITO/Ni@5AIA metallogel/Al structure. Prior to device manufacturing, soap solution, acetone, ethanol, and distilled

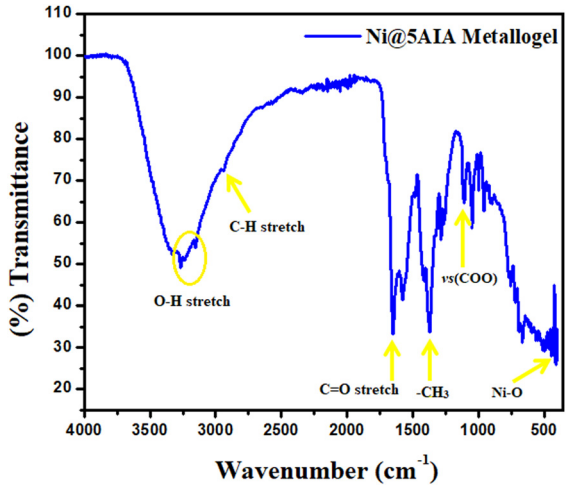

Fig. 5 FT-IR spectra of the xerogel form of Ni@5AIA metallogel.

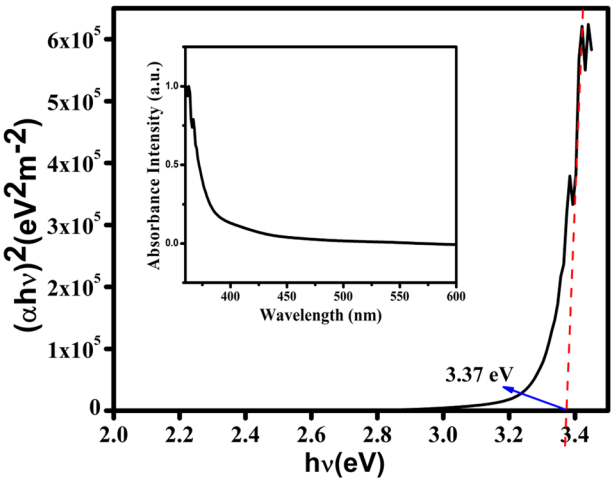

Fig. 6 $(\alpha h\gamma)^2$ *versus* $h\gamma$ curves of Ni@5AIA, UV-Vis absorption spectra (inset) were determined with the help of Tauc'sequation.

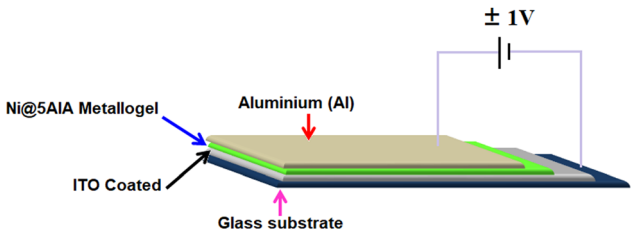

Scheme 1 Schematic diagram of MS junction device based on Ni@5AIA metallogel.

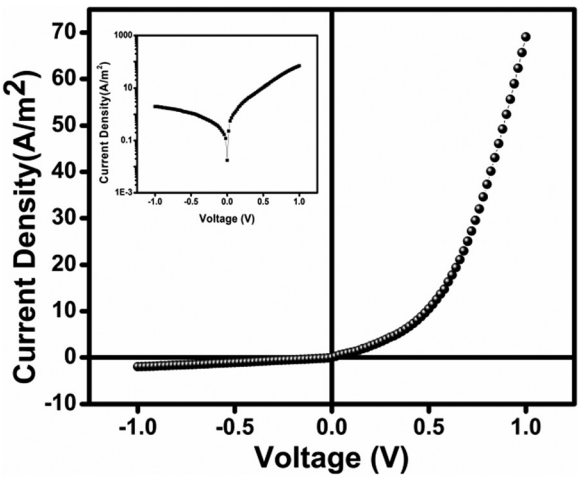

Fig. 7 Current density–voltage (*J*–*V*) graph of artificial gel under dark condition. The insets show respective *J vs. V* plots (in log scale).

water were used sequentially in an ultrasonic bath to clean and dry indium tin oxide (ITO)-coated glass substrates (Scheme 1).

3.5. Optical characterization

To measure the optical band gap we recorded the absorption spectra of the synthesized gel in the wavelength region from 360 to 600 nm using a UV-Vis spectrophotometer and the recorded spectra are shown in Fig. 6 (inset). The optical band gap was determined from the analysis of the Tauc plot using the equation

$$\alpha h\nu = A(h\nu - E_g)^n$$

where α = absorption coefficient, h = Planck's constant, ν = frequency of light, A = energy dependent constant (taken as 1), E_g = band gap, n = electron transition process dependent const (for direct transition n = 1/2). $(\alpha h\nu)^2$ *vs.* $h\nu$ plot are shown in Fig. 6 where, by the extrapolation of the linear part of the curve we can conclude that the material has a direct optical band gap of 3.37 eV.

3.6. Electrical characterization of device

We investigated the electrical properties of our synthetic gel. To explore the charge transport properties, we fabricated our synthesized gel-based thin film MS junction devices and measured current density–voltage (*J*–*V*) data within a bias range of ±1 V. The *J*–*V* characteristics of the gel-based metal–semiconductor junction device are shown in Fig. 7. Our synthetic gel-

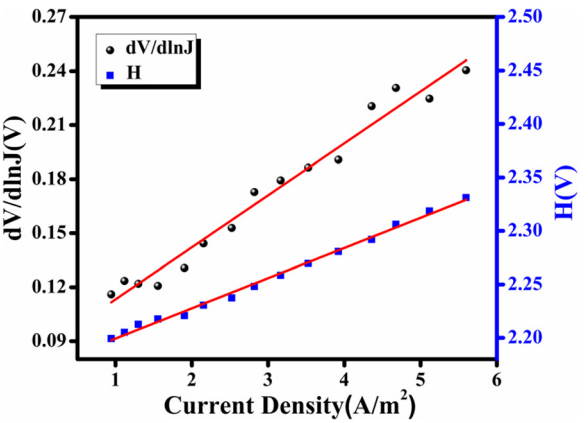

Fig. 8 Under dark conditions, d*V*/d ln *J vs. J* and *H*(*J*) *vs. J* curves in double *y* axis.

Table 1 Electrical parameters of gel based SD

Rectification ratio	Conductivity (S m^{-1})	Series resistance (Ω) from dV/d ln$J$ *vs.* J curve	Series resistance (Ω) from H *vs.* J curve	Ideality factor (η)	Barrier height φ_b (eV)
34.77	1.53×10^{-5}	4.17 K	3.99 K	3.18	0.68

Table 2 Comparison table of electrical parameters of Ni(II)-metallogel based device with other reported results

Device based on	Rectification ratio	Conductivity (S m^{-1})	Ideality factor (η)	Barrier height (φ_B) (eV)	Series resistance R_S (Ohm) dV/d ln$J$ *vs.* J	Series resistance R_S (Ohm) $H(J)$ *vs.* J	Ref.
Ni(II)-metallogel	34.77	1.53×10^{-5}	3.18	0.68	4170	3990	This work
Cd-CADS	19.51	1.49×10^{-5}	0.61	0.62	2372	2220	67
Cd-N_2H_4	23.53	2.04×10^{-6}	3.01	0.47	6730	6640	6*h*
$C_{40}H_{34}Cu_2N_6O_{18}$	8.46	2.02×10^{-6}	2.78	0.47	81.7	84.3	68
$C_{20}H_{18}CuN_2O_{10}$	8.49	2.34×10^{-6}	2.08	0.44	50 150	53 170	68
Zn@TA	37.06	7.77×10^{-6}	3.78	0.47	3751.26	3587.73	69
Ni-SA	21.54	11.16×10^{-6}	1.79	0.66	1700	1880	70
Zn-SA	20.83	6.72×10^{-6}	2.53	0.70	2890	3000	70
Cd-SA	20.11	4.02×10^{-6}	2.61	0.73	4110	4170	70
Ni-SB	1.64	2.62×10^{-6}	3.00	0.74	18 900	18 830	71
Zn-SB	14.63	1.18×10^{-6}	3.93	0.75	37 340	3930	71
Fe-metallogel	42.19	4.53×10^{-6}	2.92	0.78	14 080	13 420	72
$[(NiLB)_2(SCN)_2Mn]$	—	5.29×10^{-6}	1.22	0.70	4025	3016	73

based device has an approximate conductivity of 1.53×10^{-5} S m^{-1}, similar to that of a semiconductor. The measured J–V curve of the gel-based device shows that it has good rectifying properties, establishing Schottky diode (SD) behavior. The correction ratio (J_{on}/J_{off}) of the gel-based SD was determined as 34.77 based on the JV characteristic at ± 1 V.

To examine the J–V characteristics obtained in this case, we used the thermionic emission theory and applied the technique proposed by Cheung to extract some key diode parameters.[63] The following general equations were used to initiate the analysis of the J–V curve:[63,64]

$$J = J_0\left[\exp\left(\frac{qV}{\eta KT}\right) - 1\right] \quad (1)$$

$$J_0 = \text{saturation current density} = A^* T^2 \exp\left(-\frac{q\Phi_B}{KT}\right) \quad (2)$$

Each parameter has its conventional interpretation. We also calculated the series resistance, ideality factor, and impedance potential height using eqn (3) and (4).[64,65]

$$\frac{dV}{d\ln J} = AJR_S + \frac{\eta KT}{q} \quad (3)$$

$$H(J) = V - \frac{\eta KT}{q}\ln\left(\frac{J}{A^* T^2}\right) = AJR_S + \eta\Phi_B \quad (4)$$

For complex-based devices, the ideality factor (η) was calculated from the intercept of the dV/d(ln$J$) *vs.* J plot, while the barrier height was calculated from the intercept of the H *vs.* J plot (Fig. 8). The calculated ideality factor value shows that the MS junction is not behaving ideally. This departure from the ideal value may be primarily due to impedance height, the presence of series resistance, and inhomogeneity of MS junction interface conditions.[66] The series resistance (R_S) was determined using the slope of the H *vs.* J and dV/d(ln$J$) *vs.* J plots (Fig. 8). Table 1 provides an overview of the estimated barrier potential height (φ_B), series resistance (R_S), and ideality factor (η) for the synthesised complex-based SD. The results shown in the table indicate clearly that both approaches (eqn (3) and (4)) employing Cheung's functions produce results that are very similar. The synthesized complex can play an important role in the development of metallogel-based semiconductor devices, according to all measured parameters.

The parameters of our fabricated semiconductor device were then compared with various other reported semiconductor devices and the results are presented in Table 2. From Table 2, it is clear that our synthesized Ni(II)-metallogel has greater electrical conductivity than other materials reported.

4. Conclusions

Briefly, a novel supramolecular Ni(II)-metallogel based on 5-aminoisophthalic acid gelator was prepared by immediate mixing of nickel acetate and 5-aminoisophthalic acid in DMF followed by sonication at room temperature. Various non-covalent interactions contribute to the formation of stable Ni@5AIA metallogels at room temperature. The FESEM microstructural analysis of the Ni@5AIA metallogel revealed a flake-like hierarchical architecture of the hydrogel. The mechanical stability of the Ni@5AIA metallogel material was verified by rheological tests. Optical band-gap measurements of our synthesized Ni@5AIA metallogel suggest the semiconducting nature of the metallogel. In addition, a metal–semiconductor

junction thin film device was fabricated using Au metal and semiconducting Ni@5AIA metallogel. The nonlinear charge transport of the device obtained from the *I–V* characteristic graph confirmed the fabrication of a Schottky diode. Thus, the present study of a sandwich-like configuration of ITO/Ni@5AIA metallogel/Au suggests the future possibility of achieving supramolecular Ni^{2+} metallogel based electronic devices for advanced technology. Indeed, this study on Ni@5AIA metallogel based on 5-aminoisophthalic acid and a nickel(II) source indicates a pioneering method and metallogel for the fabrication of semiconducting devices.

Conflicts of interest

The authors declare no competing financial interests.

Acknowledgements

S. D. is grateful to the UGC, New Delhi, for awarding him Dr DS Kothari Postdoctoral Fellowship (Award letter number: No. F.4-2/2006 (BSR)/CH/19-20/0224). S. B. gratefully acknowledges DST Inspire Faculty Research Grant (Faculty Registration No. IFA18-CH304; DST/INSPIRE/04/2018/000329).

Notes and references

1 R. Kuosmanen, K. Rissanen and E. Sievänen, *Chem. Soc. Rev.*, 2020, **49**, 1977–1998.
2 G. M. Whitesides, J. P. Mathias and C. T. Seto, *Science*, 1991, **254**, 1312–1319.
3 J. W. Steed, *Chem. Commun.*, 2011, **47**, 1379–1383.
4 P. Dastidar, *Chem. Soc. Rev.*, 2008, **37**, 2699–2715.
5 S. Dhibar, A. Dey, S. Majumdar, D. Ghosh, P. P. Ray and B. Dey, *ACS Appl. Electron. Mater.*, 2019, **1**, 1899–1908.
6 (*a*) S. Dhibar, D. Ghosh, S. Majumdar and B. Dey, *ACS Omega*, 2020, **5**, 2680–2689; (*b*) S. Dhibar, A. Dey, R. Jana, A. Chatterjee, G. K. Das, P. P. Ray and B. Dey, *Dalton Trans.*, 2019, **48**, 17388–17394; (*c*) S. Dhibar, R. Jana, P. P. Ray and B. Dey, *J. Mol. Liq.*, 2019, **289**, 111–126; (*d*) S. Dhibar, A. Dey, D. Ghosh, A. Mandal and B. Dey, *J. Mol. Liq.*, 2019, **276**, 184–193; (*e*) S. Dhibar, A. Dey, A. Dey, S. Majumdar, A. Mandal, P. P. Ray and B. Dey, *New J. Chem.*, 2019, **43**, 15691–15699; (*f*) D. Ghosh, S. Dhibar, A. Dey, S. Mukherjee, N. Joardar, S. P. Sinha Babu and B. Dey, *J. Mol. Liq.*, 2019, **280**, 1–12; (*g*) S. Majumdar, T. Singha, S. Dhibar, A. Mandal, P. K. Datta and B. Dey, *ACS Appl. Electron. Mater.*, 2020, **2**, 3678–3685; (*h*) S. Majumdar, A. Dey, R. Sahu, S. Dhibar, P. P. Ray and B. Dey, *ACS Appl. Nano Mater.*, 2020, **3**, 11025–11036.
7 (*a*) C. Po, Z. Ke, A. Y. Y. Tam, H. F. Chow and V. W. W. Yam, *Chem. – Eur. J.*, 2013, **19**, 15735–15744; (*b*) S. Ganta and D. K. Chand, *Inorg. Chem.*, 2018, **57**, 3634–3645; (*c*) P. Chen, Q. Li, S. Grindy and N. Holten-Andersen, *J. Am. Chem. Soc.*, 2015, **137**, 11590–11593.
8 (*a*) Q. Lin, Q.-P. Yang, B. Sun, Y.-P. Fu, X. Zhu, T.-B. Wei and Y.-M. Zhang, *Soft Matter*, 2014, **10**, 8427–8432; (*b*) A. M. Amacher, J. Puigmartí-Luis, Y. Geng, V. Lebedev, V. Laukhin, K. Kramer, J. Hauser, D. B. Amabilino, S. Decurtins and S.-X. Decurtins, *Chem. Commun.*, 2015, **51**, 15063–15066; (*c*) S. Sarkar, S. Dutta, P. Bairi and T. Pal, *Langmuir*, 2014, **30**, 7833–7841.
9 (*a*) C. K. Karan and M. Bhattacharjee, *ACS Appl. Mater. Interfaces*, 2016, **8**, 5526–5535; (*b*) S. Dey, D. Datta, K. Chakraborty, S. Nandi, A. Anoop and T. Pathak, *RSC Adv.*, 2013, **3**, 9163–9166; (*c*) M.-O. M. Piepenbrock, N. Clarke and J. W. Steed, *Soft Matter*, 2010, **6**, 3541–3547; (*d*) M.-O. M. Piepenbrock, N. Clarke and J. W. Steed, *Langmuir*, 2009, **25**, 8451–8456.
10 (*a*) Z. Yao, Z. Wang, Y. Yu, C. Zeng and K. Cao, *Polymer*, 2017, **119**, 98–106; (*b*) P. Rajamalli, P. Malakar, S. Atta and E. Prasad, *Chem. Commun.*, 2014, **50**, 11023–11025.
11 K. Mitsumoto, J. M. Cameron, R.-J. Wei, H. Nishikawa, T. Shiga, M. Nihei, G. N. Newton and H. Oshio, *Chem. – Eur. J.*, 2017, **23**, 1502–1506.
12 X.-Q. Wang, W. Wang, G.-Q. Yin, Y.-X. Wang, C.-W. Zhang, J.-M. Shi, Y. Yu and H.-B. Yang, *Chem. Commun.*, 2015, **51**, 16813–16816.
13 B. Jiang, L.-J. Chen, G.-Q. Yin, Y.-X. Wang, W. Zheng, L. Xu and H.-B. Yang, *Chem. Commun.*, 2017, **53**, 172–175.
14 (*a*) F. Gou, J. Cheng, X. Zhang, G. Shen, X. Zhou and H. Xiang, *Eur. J. Inorg. Chem.*, 2016, 4862–4866; (*b*) N. Kelly, K. Gloe, T. Doert, F. Hennersdorf, A. Heine, J. Marz, U. Schwarzenbolz, J. J. Weigand and K. J. Gloe, *Organomet. Chem.*, 2016, **821**, 182–191.
15 (*a*) S. Dhibar, A. Dey, S. Majumdar, D. Ghosh, A. Mandal, P. P. Ray and B. Dey, *Dalton Trans.*, 2018, **47**, 17412–17420; (*b*) S. Dhibar, A. Dey, D. Ghosh, S. Majumdar, A. Dey, P. Mukherjee, A. Mandal, P. P. Ray and B. Dey, *ChemistrySelect*, 2019, **4**, 1535–1541; (*c*) S. Dhibar, A. Dey, S. Majumdar, A. Dey, P. P. Ray and B. Dey, *Ind. Eng. Chem. Res.*, 2020, **59**, 5466–5473; (*d*) S. Dhibar, A. Dey, S. Majumdar, P. P. Ray and B. Dey, *Int. J. Energy Res.*, 2021, **45**, 5486–5499; (*e*) S. Dhibar, S. K. Ojha, A. Mohan, S. P. C. Prabhakaran, S. Bhattacharjee, K. Karmakar, P. Karmakar, P. Predeep, A. K. Ojha and B. Saha, *New J. Chem.*, 2022, **46**, 17189–17200; (*f*) S. Dhibar, H. Dahiya, K. Karmakar, S. Kundu, S. Bhattacharjee, G. C. Nayak, P. Karmakar, G. D. Sharma and B. Saha, *J. Mol. Liq.*, 2023, **370**, 121020; (*g*) S. Dhibar, A. Dey, A. Dalal, S. Bhattacharjee, R. Sahu, R. Sahoo, A. Mondal, S. M. Rahaman, S. Kundu and B. Saha, *J. Mol. Liq.*, 2023, **370**, 121021; (*h*) S. Dhibar, S. Babu, A. Mohan, G. K. Chandra, S. Bhattacharjee, K. Karmakar, P. Karmakar, S. M. Rahaman, P. Predeep and B. Saha, *J. Mol. Liq.*, 2023, **375**, 121348; (*i*) K. Karmakar, A. Dey, S. Dhibar, R. Sahu, S. Bhattacharjee, P. Karmakar, P. Chatterjee, A. Mondal and B. Saha, *RSC Adv.*, 2023, **13**, 2561–2569; (*j*) S. Dhibar, B. Pal, K. Karmakar, S. Kundu, S. Bhattacharjee, R. Sahoo, S. M. Rahaman, D. Dey, P. P. Ray and B. Saha, *ChemistrySelect*, 2023, **8**, e202204214.
16 (*a*) Z. Yao, Z. Wang, Y. Yu, C. Zeng and K. Cao, *Polymer*, 2017, **119**, 98–106; (*b*) P. Rajamalli, P. Malakar, S. Atta and E. Prasad, *Chem. Commun.*, 2014, **50**, 11023–11025.

17 (*a*) S. Ganta and D. K. Chand, *Dalton Trans.*, 2015, **44**, 15181–15188; (*b*) L. Yang, L. Luo, S. Zhang, X. Su, J. Lan, C.-T. Chen and J. You, *Chem. Commun.*, 2010, **46**, 3938–3940; (*c*) B. Xing, M.-F. Choi, Z. Zhou and B. Xu, *Langmuir*, 2002, **18**, 9654–9658; (*d*) X. Ma, S. Liu, Z. Zhang, Y. Niu and J. Wu, *Soft Matter*, 2017, **13**, 8882–8885.
18 C. A. Offiler, C. D. Jones and J. W. Steed, *Chem. Commun.*, 2017, **53**, 2024–2027.
19 X. Yu, Z. Wang, Y. Li, L. Geng, J. Ren and G. Feng, *Inorg. Chem.*, 2017, **56**, 7512–7518.
20 M. Suzuki and K. Hanabusa, *Chem. Soc. Rev.*, 2010, **39**, 455–463.
21 P. Terech and R. G. Weiss, *Chem. Rev.*, 1997, **97**, 3133–3159.
22 J. Raeburn and D. J. Adams, *Chem. Commun.*, 2015, **51**, 5170–5180.
23 S. J. Wezenberg, C. M. Croisetu, M. C. A. Stuartab and B. L. Feringa, *Chem. Sci.*, 2016, **7**, 4341–4346.
24 N. Shi, G. Yin, H. Li, M. Hana and Z. Xu, *New J. Chem.*, 2008, **32**, 2011–2015.
25 K. Hanabusa, K. Hiratsuka, M. Kimura and H. Shirai, *Chem. Mater.*, 1999, **11**, 649–655.
26 J. W. Steed, *Chem. Soc. Rev.*, 2010, **39**, 3686–3699.
27 C. Tomasini and N. Castellucci, *Chem. Soc. Rev.*, 2013, **42**, 156–172.
28 A. Prathap and K. M. Sureshan, *Langmuir*, 2019, **35**, 6005–6014.
29 D. K. Smith, *Adv. Mater.*, 2006, **18**, 2773–2778.
30 R. G. Weiss and P. Terech, *Molecular Gels: Materials with Self-Assembled Fibrillar Networks*, Springer, Dordrecht, 2005.
31 (*a*) T.-A. Asoh and A. Kikuchi, *Chem. Commun.*, 2012, **48**, 10019–10021; (*b*) X. Wang, F. Liu, X. Zheng and J. Sun, *Angew. Chem., Int. Ed.*, 2011, **50**, 11378–11381; (*c*) H. Wang, M. B. Hansen, D. W. P. M. Löwik, J. C. M. van Hest, Y. Li, J. A. Jansen and S. C. G. Leeuwenburgh, *Adv. Mater.*, 2011, **23**, H119–H124.
32 (*a*) A. Y.-Y. Tam and V. W.-W. Yam, *Chem. Soc. Rev.*, 2013, **42**, 1540–1567; (*b*) C. Tomasini and N. Castellucci, *Chem. Soc. Rev.*, 2013, **42**, 156–172; (*c*) L. Meazza, J. A. Foster, K. Fucke, P. Metrangolo, G. Resnati and J. W. Steed, *Nat. Chem.*, 2013, **5**, 42–47.
33 (*a*) M. Shirakawa, N. Fujita and S. Shinkai, *J. Am. Chem. Soc.*, 2003, **125**, 9902–9903; (*b*) J. R. Moffat, G. J. Seeley, J. T. Carter, A. Burgess and D. K. Smith, *Chem. Commun.*, 2008, 4601–4603.
34 (*a*) Y. Xu, Q. Wu, Y. Sun, H. Bai and G. Shi, *ACS Nano*, 2010, **4**, 7358–7362; (*b*) S. Burattini, B. W. Greenland, D. H. Merino, W. Weng, J. Seppala, H. M. Colquhoun, W. Hayes, M. E. Mackay, I. W. HamLey and S. J. Rowan, *J. Am. Chem. Soc.*, 2010, **132**, 12051–12058.
35 W. Fang, Y. Zhang, J. Wu, C. Liu, H. Zhu and T. Tu, *Chem. – Asian J.*, 2018, **13**, 712–729.
36 J. Kim, J. A. Hanna, M. Byun, C. D. Santangelo and R. C. Hayward, *Science*, 2012, **335**, 1201–1205.
37 A. R. Hirst, B. Escuder, J. F. Miravet and D. K. Smith, *Angew. Chem., Int. Ed.*, 2008, **47**, 8002–8018.
38 X. Cheng, J. Pan, Y. Zhao, M. Liao and H. Peng, *Adv. Energy Mater.*, 2018, **8**, 1702184.
39 (*a*) S. Sarkar, S. Dutta, S. Chakrabarti, P. Bairi and T. Pal, *ACS Appl. Mater. Interfaces*, 2014, **6**, 6308–6316; (*b*) Q. Lin, T.-T. Lu, X. Zhu, B. Sun, Q.-P. Yang, T.-B. Wei and Y.-M. Zhang, *Chem. Commun.*, 2015, **51**, 1635–1638.
40 W. Wang, H. Wang, C. Ren, J. Wang, M. Tan, J. Shen, Z. Yang, P. G. Wang and L. Wang, *Carbohydr. Res.*, 2011, **346**, 1013–1017.
41 M. R. Saboktakin and R. M. Tabatabaei, *Int. J. Biol. Macromol.*, 2015, **75**, 426–436.
42 Y. Zhao, S. Song, X. Ren, J. Zhang, Q. Lin and Y. Zhao, *Chem. Rev.*, 2022, **122**, 5604–5640.
43 W.-L. Guan, K. M. Adam, M. Qiu, Y.-M. Zhang, H. Yao, T.-B. Wei and Q. Lin, *Supramol. Chem.*, 2020, **32**, 578–596.
44 W. H. Binder, L. Petraru, T. Roth, P. W. Groh, V. Pálfi, S. Keki and B. Ivan, *Adv. Funct. Mater.*, 2007, **17**, 1317–1326.
45 A. Khan, R. R. Kisannagar, C. Gouda, D. Gupta and H.-C. Lin, *J. Mater. Chem. A*, 2020, **8**, 19954–19964.
46 B. Xue, M. Qin, T. Wang, J. Wu, D. Luo, Q. Jiang, Y. Li, Y. Cao and W. Wang, *Adv. Funct. Mater.*, 2016, **26**, 9053–9062.
47 B. Zhang and J. N. H. Reek, *Chem. – Asian J.*, 2021, **16**, 3851–3863.
48 S. Biswas, U. Chatterjee, S. Sarkar, F. Khan, D. Bera, M. Mukhopadhyay, S. Goswami, S. Chakrabarti and S. Das, *Colloids Surf., B*, 2020, **188**, 110803.
49 N. Kelly, K. Gloe, T. Doert, F. Hennersdorf, A. Heine, J. Maerz, U. Schwarzenbolz, J. J. Weigand and K. Gloe, *J. Organomet. Chem.*, 2016, **821**, 182–191.
50 L. Yan, C. Liu, L. Shen, J. Li, X. Liu, M. Lv, C. Su and Z. Ye, *Chem. Lett.*, 2018, **47**, 640–642.
51 J. H. Lee, Y. E. Baek, K. Y. Kim, H. Choi and J. H. Jung, *Supramol. Chem.*, 2016, **28**, 870–873.
52 S. Dhibar, S. K. Ojha, K. Karmakar, P. Karmakar, S. Bhattacharjee, P. Chatterjee, A. K. Ojha and B. Saha, *Chem. Afr.*, 2023, DOI: **10.1007/s42250-023-00680-w**.
53 J. Chen, T. Wang and M. Liu, *Inorg. Chem. Front.*, 2016, **3**, 1559–1565.
54 J.-L. Zhong, X.-J. Jia, H.-J. Liu, X.-Z. Luo, S.-G. Hong, N. Zhang and J.-B. Huang, *Soft Matter*, 2016, **12**, 191–199.
55 L. Arnedo-Sánchez, S. Bhowmik, S. Hietala, R. Puttreddy, M. Lahtinen, L. D. Cola and K. Rissanen, *Dalton Trans.*, 2017, **46**, 7309–7316.
56 X. Li, J. Shi, Y. Gao, H.-C. Lin and B. Xu, *J. Am. Chem. Soc.*, 2011, **133**, 17513–17518.
57 V. Singh, S. Kala, T. Rom, A. K. Paul and R. Pandey, *Dalton Trans.*, 2023, **52**, 7088–7103.
58 H. Guo, Q. Feng, K. Xu, J. Xu, J. Zhu, C. Zhang and T. Liu, *Adv. Funct. Mater.*, 2019, **29**, 1903660.
59 G. Lepcha, T. Singha, S. Majumdar, A. K. Pradhan, K. S. Das, P. K. Datta and B. Dey, *Dalton Trans.*, 2022, **51**, 13435–13443.
60 P. Terech, M. Yan, M. Maréchal, G. Royal, J. Galveza and S. K. P. Velu, *Phys. Chem. Chem. Phys.*, 2013, **15**, 7338–7344.
61 N. Malviya, C. Sonkar, B. K. Kundu and S. Mukhopadhyay, *Langmuir*, 2018, **34**, 11575–11585.

62 (*a*) E. M. M. Ibrahim, L. H. Abdel-Rahman, A. M. Abu-Dief, A. Elshafaie, S. K. Hamdan and A. M. Ahmed, *Mater. Res. Bull.*, 2018, **107**, 492–497; (*b*) A. Elshafaie, L. H. Abdel-Rahman, A. M. Abu-Dief, S. K. Hamdan, A. M. Ahmed and E. M. M. Ibrahim, *NANO*, 2018, **13**, 1850074; (*c*) L. H. Abdel Rahman, A. M. Abu-Dief, R. M. El-Khatib, S. M. Abdel-Fatah, A. M. Adam and E. M. M. Ibrahim, *Appl. Organomet. Chem.*, 2018, **32**, e4174; L. H. Abdel Rahman, A. M. Abu-Dief, R. M. El-Khatib, S. M. Abdel-Fatah, A. M. Adam and E. M. M. Ibrahim, *Appl. Organomet. Chem.*, 2018, **32**, e4174.

63 R. Jana, S. Sil, A. Dey, J. Datta and P. P. Ray, *AIP Adv.*, 2018, **8**, 125104.

64 J. Datta, A. Dey, S. K. Neogi, M. Das, S. Middya, R. Jana, S. Bandopadhyay, A. Layek and P. P. Ray, *IEEE Trans. Electron Devices*, 2017, **64**, 4724–4730.

65 S. K. Cheung and N. W. Cheung, Extraction of Schottky diode parameters from forward current-Voltage characteristics, *Appl. Phys. Lett.*, 1986, **49**, 85–87.

66 J. Datta, M. Das, S. Sil, S. Kumar, A. Dey, R. Jana, S. Bandyopadhyay and P. P. Ray, *Mater. Sci. Semicond. Process.*, 2019, **91**, 133–145.

67 S. Majumdar, B. Pal, R. Sahu, K. S. Das, P. P. Ray and B. Dey, *Dalton Trans.*, 2022, **51**, 9007–9016.

68 A. Hossain, A. Dey, S. K. Seth, P. P. Ray, P. Ballester, R. G. Pritchard, J. Ortega-Castro, A. Frontera and S. Mukhopadhyay, *ACS Omega*, 2018, **3**, 9160–9171.

69 S. Majumdar, A. Dey, R. Sahu, G. Lepcha, A. Dey, P. P. Ray and B. Dey, *Mater. Res. Bull.*, 2023, **157**, 112003.

70 G. Lepcha, S. Majumdar, B. Pal, K. T. Ahmed, I. Pal, B. Satpati, S. R. Biswas, P. P. Ray and B. Dey, *Langmuir*, 2023, **39**, 7469–7483.

71 G. Lepcha, B. Pal, S. Majumdar, K. T. Ahmed, I. Pal, S. R. Biswas, P. P. Ray and B. Dey, *Mater. Adv.*, 2023, **4**, 2595–2603.

72 S. Saha, B. Pal, K. S. Das, P. K. Ghose, A. Ghosh, A. De, A. K. Das, P. P. Ray and R. Mondal, *ChemistrySelect*, 2022, **7**, e202203307.

73 M. Das, M. Das, S. Ray, U. K. Das, S. Laha, P. P. Ray, B. C. Samanta and T. Maity, *New J. Chem.*, 2022, **46**, 21103–21114.